Optics Letters

Intensity noise manipulation of a single-frequency laser with high output power by intracavity nonlinear loss

HUADONG LU,* YONGRUI GUO, AND KUNCHI PENG

State Key Laboratory of Quantum Optics and Quantum Optics Devices, Institute of Opto-Electronics, Shanxi University, Taiyuan, Shanxi 030006, China
**Corresponding author: luhuadong@sxu.edu.cn*

Received 4 September 2015; revised 7 October 2015; accepted 8 October 2015; posted 12 October 2015 (Doc. ID 249264); published 4 November 2015

The influences of intracavity nonlinear losses on the intensity noise of output lasers are theoretically and experimentally investigated with an all-solid-state single-frequency laser with high gain. By means of tuning the temperature of a nonlinear crystal deliberately placed inside the laser resonator, the intracavity nonlinear loss of the laser is controlled. The dependence of the frequency and amplitude of the resonant relaxation oscillation peak on the nonlinear loss is studied in detail for both fundamental-wave (FW) and second-harmonic-wave (SHW). We find that, by controlling the temperature of the nonlinear crystal, the intensity noises of the laser can be transferred between FW and SHW. The theoretical predictions are in good agreement with the experimental measurements. The obtained results can be applied to manipulate and suppress the laser noises. © 2015 Optical Society of America

OCIS codes: (270.2500) Fluctuations, relaxations, and noise; (140.3515) Lasers, frequency doubled; (140.3560) Lasers, ring; (140.3570) Lasers, single-mode.

http://dx.doi.org/10.1364/OL.40.005196

All-solid-state continuous-wave (CW) single-frequency lasers at 1064 nm are of great interest for many applications, including optical parametric oscillators (OPO), atomic trapping, gravitation-wave detection, quantum optics owing to their intrinsic advantages of narrow linewidth, and good beam quality in conjunction with extremely low intensity noise. For obtaining a single-frequency laser with high output power and perfect beam quality to satisfy the requirements of various applications, Martin *et al.* presented a feasible method recently in which the nonlinear loss was introduced into a ring resonator of traveling-wave operation [1]. It had been demonstrated that, when the nonlinear loss was deliberately introduced into a laser resonator, the nonlinear loss lasing modes were half that of nonlasing modes, and the loss difference between lasing and nonlasing modes equaled the second-harmonic conversion efficiency [1]. Applying this effect, the oscillation of the nonlasing modes was effectively suppressed, and the single-frequency operation of the laser was realized. Then, Greenstein and Rosenbluh [2] investigated the influence of the nonlinear spectral bandwidth on the mode stability in 2005. Our group theoretically and experimentally studied the physical conditions of single-frequency operation for all-solid-state lasers with high output power in 2014 [3]. We pointed out that the laser can work in the state of the single-frequency operation if and only if the nonlinear loss induced by the intracavity nonlinear crystal is larger than a certain value. Then, we achieved a broadband tunable laser by using the intracavity nonlinear loss to replace the traditional intravavity locked elements [4,5]. In the above experiments, the intensity noise reduction of the laser was observed due to the introduction of the nonlinear loss; however, the careful research on the phenomenon was not implemented. In 2015, Amili and Alouini suppressed the resonant intensity noise in solid-state lasers using a second-harmonic generation (SHG)-based buffer reservoir [6]. In their system, the nonlinear loss induced by the SHG was very small and, thus, the process of the SHG hardly affected the output power of the main infrared (IR) laser. However, for suppressing the multi-longitudinal-mode (MLM) oscillation in a laser with high gain, the intracavity nonlinear loss has to be increased to a required value. In this case, the large nonlinear loss will directly effect the output power of the main IR laser. A detailed study about the influences of the nonlinear loss on the intensity noise of lasers has not been presented so far to the best of our knowledge. In this Letter, we will investigate the effect of the nonlinear loss on the intensity noise of a laser with high gain theoretically and experimentally. We find that the intensity noise spectra of a laser can be manipulated by the intracavity nonlinear loss.

The transfer-function-type theory explicitly shows the origin of noises by solving the quantum Langevin equation around its steady-state solution in the case of existing various external quantum-mechanical reservoirs [7]. The origin of noises includes vacuum noise V_{vac} entering at the output coupler, intensity noise V_p of the pump source, spontaneous-emission noise V_{spont}, dipole fluctuation noise V_{dipole}, and noise introduced from intracavity losses V_{losses}. The photon decay rates

induced by the output losses and intracavity losses are expressed as $2\kappa_m$ and $2\kappa_l$, respectively. When the nonlinear loss is deliberately introduced to the resonator of the laser, the photon decay rate induced by the nonlinear loss ($2\kappa_n$) equals [8]

$$2\kappa_n = 2\,\mu\alpha^2, \tag{1}$$

where μ is the nonlinear conversion rate and α^2 is the intracavity photon number. The total photon decay rate is

$$2\kappa_t = 2\kappa_m + 2\kappa_l + 2\kappa_n. \tag{2}$$

The laser rate equations are given by

$$\begin{aligned}
\dot{a} &= \frac{G}{2}(J_3 - J_2)\alpha - (\kappa_l + \kappa_m + \kappa_n)\alpha,\\
\dot{J}_1 &= -\Gamma J_1 + \gamma J_2,\\
\dot{J}_2 &= G(J_3 - J_2)\alpha^2 + \gamma_t J_3 - \gamma J_2,\\
\dot{J}_3 &= -G(J_3 - J_2)\alpha^2 - \gamma_t J_3 + \Gamma J_1,
\end{aligned} \tag{3}$$

where G is the stimulated-emission absorption rate per photon; Γ is the pump rate; γ_t and γ are the atomic spontaneous emission rates from level $|3\rangle$ to $|2\rangle$ and $|2\rangle$ to $|1\rangle$, respectively; and J_1, J_2, and J_3 are the expectation values of the atomic populations of level $|1\rangle$, $|2\rangle$ and $|3\rangle$, respectively. The equations have been normalized by the atomic populations N; that is,

$$J_1 + J_2 + J_3 = 1. \tag{4}$$

From Eqs. (1)–(4), the values of the J_1, J_2, J_3, and α^2 can be calculated.

The intensity noise spectrum (V_f) of the fundamental-wave (FW) laser is expressed by [7]

$$\begin{aligned}
V_f = &\left\{\frac{[2\kappa_m^2(G\alpha^2 + \Gamma + \gamma_t) + \omega^2 - 2G\alpha^2\kappa_t]^2}{(\omega_f^2 - \omega^2)^2 + \omega^2\gamma_f^2}\right.\\
&\left.+\frac{\omega^2(2\kappa_m - G\alpha^2 - \Gamma - \gamma_t)^2}{(\omega_f^2 - \omega^2)^2 + \omega^2\gamma_f^2}\right\}V_{\text{vac1}}\\
&+\frac{4\kappa_m^2[(G\alpha^2 + \Gamma + \gamma_t)^2 + \omega^2]}{(\omega_f^2 - \omega^2)^2 + \omega^2\gamma_f^2}V_{\text{vac2}}\\
&+\frac{2\kappa_m G^2\alpha^2\Gamma J_1}{(\omega_f^2 - \omega^2)^2 + \omega^2\gamma_f^2}V_p\\
&+\frac{2\kappa_m G^2\alpha^2\gamma_t J_3}{(\omega_f^2 - \omega^2)^2 + \omega^2\gamma_f^2}V_{\text{spont}}\\
&+\frac{2\kappa_m G(J_2 + J_3)[(\gamma_t + \Gamma)^2 + \omega^2]}{(\omega_f^2 - \omega^2)^2 + \omega^2\gamma_f^2}V_{\text{dipole}}\\
&+\frac{4\kappa_m\kappa_l[(G\alpha^2 + \Gamma + \gamma_t)^2 + \omega^2]}{(\omega_f^2 - \omega^2)^2 + \omega^2\gamma_f^2}V_{\text{losses}},
\end{aligned} \tag{5}$$

where V_{vac1} and V_{vac2} are vacuum noises caused by SHG and the output coupler, respectively. The frequency of the resonant relaxation oscillation (RRO) ω_f equals

$$\omega_f = \sqrt{2\kappa_m(G\alpha^2 + \Gamma + \gamma_t) + 2G\alpha^2\kappa_t}, \tag{6}$$

and the damping rate of the oscillation γ_f is given by

$$\gamma_f = 2\kappa_m + G\alpha^2 + \gamma_t + \Gamma. \tag{7}$$

The intensity noise spectrum of the SHW is expressed by

$$\begin{aligned}
V_s = &\left\{\frac{[2\kappa_n^2(G\alpha^2 + \Gamma + \gamma_t) + \omega^2 - 2G\alpha^2\kappa_t]^2}{(\omega_s^2 - \omega^2)^2 + \omega^2\gamma_s^2}\right.\\
&\left.+\frac{\omega^2(2\kappa_n - G\alpha^2 - \Gamma - \gamma_t)^2}{(\omega_s^2 - \omega^2)^2 + \omega^2\gamma_s^2}\right\}V_{\text{vac1}}\\
&+\frac{8\kappa_n\kappa_m[(G\alpha^2 + \Gamma + \gamma_t)^2 + \omega^2]}{(\omega_s^2 - \omega^2)^2 + \omega^2\gamma_s^2}V_{\text{vac2}}\\
&+\frac{4\kappa_n G^2\alpha^2\Gamma J_1}{(\omega_s^2 - \omega^2)^2 + \omega^2\gamma_s^2}V_p\\
&+\frac{4\kappa_n G^2\alpha^2\gamma_t J_3}{(\omega_s^2 - \omega^2)^2 + \omega^2\gamma_s^2}V_{\text{spont}}\\
&+\frac{4\kappa_n G(J_2 + J_3)[(\gamma_t + \Gamma)^2 + \omega^2]}{(\omega_s^2 - \omega^2)^2 + \omega^2\gamma_s^2}V_{\text{dipole}}\\
&+\frac{8\kappa_n\kappa_l[(G\alpha^2 + \Gamma + \gamma_t)^2 + \omega^2]}{(\omega_s^2 - \omega^2)^2 + \omega^2\gamma_s^2}V_{\text{losses}},
\end{aligned} \tag{8}$$

where the frequency of the RRO ω_s is

$$\omega_s = \sqrt{2\kappa_n(G\alpha^2 + \Gamma + \gamma_t) + 2G\alpha^2\kappa_t}, \tag{9}$$

and the damping rate of the oscillation γ_s is

$$\gamma_s = 2\kappa_n + G\alpha^2 + \gamma_t + \Gamma. \tag{10}$$

According to Eqs. (5)–(10), we can calculate the RRO frequencies and peak amplitudes of FW and SHW with different nonlinear conversion rate μ, which are depicted in Figs. 1 and 2, respectively. It is obvious from Fig. 1 that both the frequency and amplitude of the RRO peak for FW decrease with the increase of the nonlinear conversion rate μ. In contrast, as shown in Fig. 2, when the nonlinear conversion rate μ increases, the RRO peak frequency of SHW moves toward higher frequency. At first, the amplitude of the RRO peak of SHW increases quickly at a small range with the increase of the nonlinear conversion rate μ; then it slowly decreases (see Fig. 2). The phenomenon shows that the resonance at ω_s in the spectrum is changed from the overdamped to the underdamped driven SHW in the process of increasing the nonlinear conversion rate μ. Comparing Figs. 1 and 2, we find that the intensity noise of the laser can be transferred from FW to SHW and, thus, the nonlinear conversion rate μ can be applied to manipulate the noise spectra of FW and SHW.

The experimental setup for implementing the intensity noise manipulation of the laser is shown in Fig. 3. The

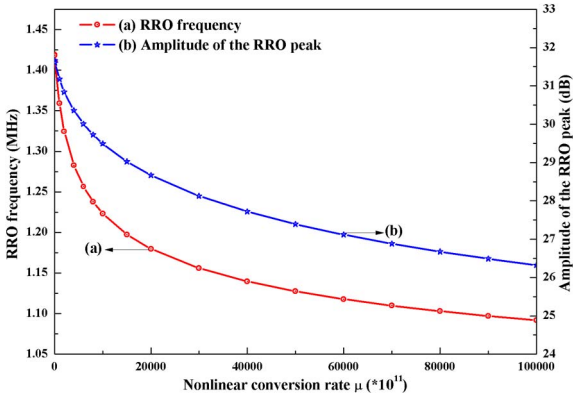

Fig. 1. Calculated RRO frequency and peak of the FW versus μ.

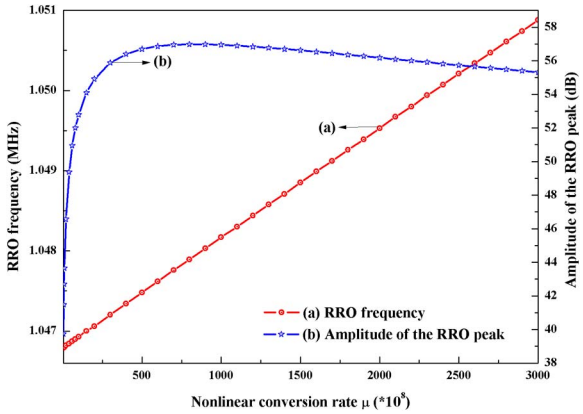

Fig. 2. Calculated RRO frequency and peak of SHW versus μ.

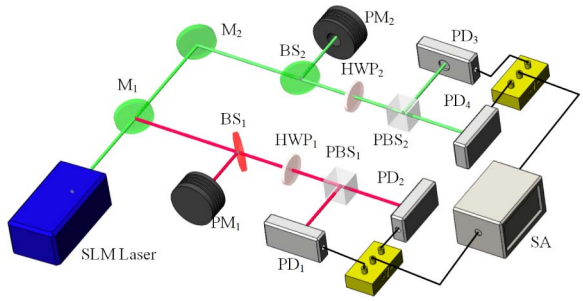

Fig. 3. Experimental setup of the noise manipulation.

configuration of the laser source used for this experiment has been presented in our previous publication [3]. The nonlinear loss is induced by an LBO nonlinear crystal with the dimensions of $3 \times 3 \times 18$ mm. The LBO crystal is cut for implementing type I noncritical phase-matched SHG and is placed at the position of the beam waist of the oscillating laser between cavity mirrors M_3 and M_4. The LBO crystal is put in a copper oven, the temperature of which is controlled at the phase-matching temperature for SHG by a homemade temperature-controller with the precision of 0.01°C (YG-2009B, YuGuang Co., Ltd.). The strength of the nonlinear loss hardly changed the impedance matching of the laser since the influence of the nonlinear crystal on the laser resonator was taken into account when the laser was designed.

The intensity noises of the 1064 and 532 nm lasers are separately measured by means of two sets of self-homodyne-detectors, each of which includes a pair of photodetectors. The photo diodes (PD, ETX500, JDSU Corporation; S3399, Hamamatsu Corporation) mounted in the photodetectors are used to measure the intensity noise of the 1064 and 532 nm lasers, respectively. The optical signals detected by two PDs are amplified by the integrated amplifiers (ADA 4817). and then the amplified photocurrents are combined with a positive/negative power combiner (±). The common mode rejection ratio of the used self-homodyne-detector (34 dB) is high enough to satisfy the requirement for implementing measurements. The sum and the subtract photocurrents stand for the intensity noise and the corresponding quantum noise limit (QNL), respectively. Finally, the noise spectra of the sum (subtract) photocurrents are analyzed by a spectral analyzer (SA) with the resolution bandwidth (RBW) of 30 kHz and the video bandwidth (VBW) of 30 Hz.

In the experiment, the nonlinear conversion rate μ was controlled by detuning the temperature of the LBO crystal. In [3,9], we found that when the temperature of the LBO crystal was changed ±2°C around the optimal phase-matching temperature, the laser still operated at the region of SLM. Once the temperature offset was more than ±2°C, the laser would start MLM oscillation. That is because the nonlinear loss was too small to suppress the oscillation of the nonlasing modes at that time. By changing the temperature of the nonlinear LBO crystal, the powers of 1064 and 532 nm lasers, as well as the longitudinal-mode structure (LMS) of the laser, are also changed. The corresponding values for four different temperatures [148.2°C (A), 149.6°C (B), 150.2°C (C), and 150.7°C (D)] are recorded in Table 1, where the power values of a 1064 nm laser stood for intracavity powers which were obtained with the output power (P_{out}) divided by the transmission of the output coupler (t) ($P_{1064} = P_{\text{out}}/t$).

The measured intensity noise spectra of a 1064 nm laser by self-homodyne-detectors for different nonlinear conversion efficiencies η at four different temperatures of the LBO crystals are shown in Fig. 4. The curves (a), (b), (c), and (d) were measured at the crystal temperatures of 148.2°C, 149.6°C, 150.2°C, and 150.7°C, respectively. The $\eta = P_{532}/P_{1064}$ was defined as the ratio between the power of 532 nm (P_{532}) and that of intracavity 1064 nm lasers (P_{1064}). A small part of the output laser power was split by a beam splitter (BS_1) and then used for the measurement of the noise spectra. The laser power injected into the homodyne detector PD_1 (PD_2) was precisely adjusted to 1 mW by a power adjuster consisting of a half-wave plate (HWP_1) and a polarizing beam splitter (PBS_1). However, when the temperature of the LBO crystal was tuned to the temperature points B, C, and D, the

Table 1. Relevant Values for Measurement of the Intensity Noise of 1064 and 532 nm Lasers

—	T(°C)	P_{1064}(W)	P_{532}(W)	η(%)	LMS
A	148.2	109.85	1.48	1.35	SLM
B	149.6	113.57	0.83	0.73	SLM
C	150.2	115.76	0.24	0.21	SLM
D	150.7	116.17	0.07	0.06	MLM

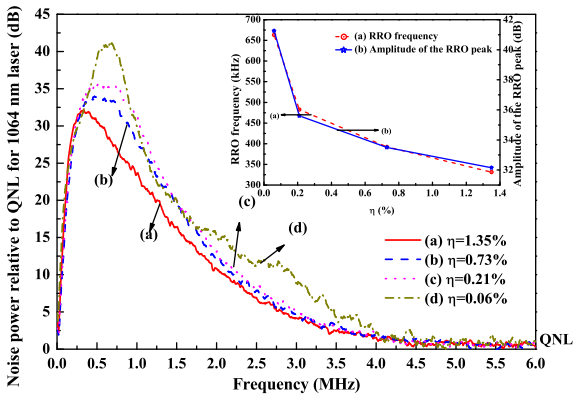

Fig. 4. Intensity noise of a 1064 nm laser with different η.

intracavity power of the 1064 nm laser increased to 113.57, 115.76, and 116.17 W, respectively, which were higher than that at point A. To compare the intensity noise of the 1064 nm laser with different η, we had to normalize the intensity noise spectra at B, C, and D points to that at point A with the relation given in [10]

$$V_{\text{obs}} = 1 + \chi(V_n - 1), \tag{11}$$

where V_{obs} and V_n expressed the observed and normalized intensity noise spectra, respectively. The χ was the normalizing factor which equaled the ratio between the intracavity powers of the 1064 nm laser at point A and that at point B, C, and D.

Figure 4 shows that the RRO peak value increases from 32 to 42 dB when the nonlinear conversion efficiency η decreases from 1.35% to 0.06% and, when the nonlinear conversion efficiency η is lower than 0.21%, the intensity noise of the 1064 nm laser at the frequency higher than RRO also increases; that is because the laser has operated in the region of MLM. The RRO peak shifts toward the high frequency with the decrease of the nonlinear conversion efficiency η. The functions of the frequency (a) and amplitude (b) of the RRO peak versus η for a 1064 nm laser are shown in inset of the Fig. 4. The experimental results are in good agreement with the theoretical predictions shown in Fig. 1.

While the intensity noise spectra of the 1064 nm laser were being measured, the intensity noise spectra of the 532 nm laser were also measured by means of another set of self-homodyne-detector, simultaneously. The experimental results are shown in Fig. 5. To implement the intensity noise spectra measurement of the 532 nm laser, the powers injected into the homodyne detectors (PD_3 and PD_4) were precisely adjusted to 2.23 mW. Likewise, the intensity noise spectra of the 532 nm at points B, C, and D were normalized to that at point A. The functions of the frequency and amplitude of the RRO peak for 532 nm laser versus η were recorded in the inset of the Fig. 5. The intensity noise spectra of the 532 nm laser had the same shapes as those of the 1064 nm laser. However, both the RRO peak and frequency gradually declined and shifted to the low frequencies with the decrease of the nonlinear loss (see the inset of Fig. 5). Comparing Figs. 2 and 5, we can see that the experimental results are also in good agreement with the theoretical expectation. Because the nonlinear conversion coefficient of the nonlinear LBO crystal was very small, the RRO peak decline of the SHW was not observed. When the nonlinear loss is lower than 0.21%, another RRO peak appears together with the main peak, which results from the oscillation of the other modes. In this experiment, we did not consider the second RRO peak and, thus, it is not marked in the insets of Fig. 4 and5. Analyzing Figs. 4 and 5, it is seen that the intensity noise can transfer from a 1064 nm laser into a 532 nm laser when the nonlinear crystal is inserted into the resonator, and the transfer degree is decided by the nonlinear loss induced by the intracavity nonlinear crystal. Thus, it shows that the intensity noise of FW and SHW can be manipulated by controlling the intracavity nonlinear loss.

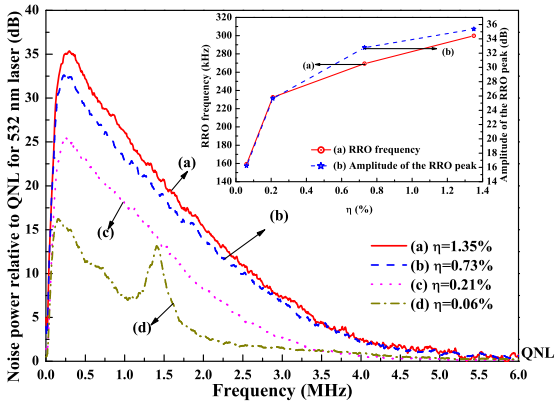

Fig. 5. Intensity noise of a 532 nm laser with different η.

In summary, we theoretically and experimentally investigated the influence of the nonlinear loss on the intensity noise of a single-frequency laser with high output power. The experiment is implemented in a homemade SLM 1064 nm laser with the intracavity nonlinear LBO crystal. When the temperature of the nonlinear crystal is tuned away from the optimal phase-matching value, the nonlinear loss decreases and the RRO peak of a 1064 nm laser increases and shifts toward the high frequencies. On the contrary, both the RRO peak and frequency of the 532 nm laser gradually decline and shift toward low frequencies with the decrease of the nonlinear loss. Comparing the intensity noise spectra of 1064 and 532 nm lasers, it is pointed out that the intensity noise can be transferred between a 1064 nm laser and a 532 nm laser when the nonlinear loss is introduced into the resonator. The results can be applied to implement the noise manipulation of FW and SHW lasers in an all-solid-state laser. The investigation tells us that a nonlinear crystal inserted into the resonator cannot serve as a noise eater; its role is to transfer the intensity noise from FW to SHW by the nonlinear conversion. The method mentioned in the letter can be used to manipulate and suppress the RRO peak of the laser that is just the role of traditional injection locking. Thus, the intracavity nonlinear loss can at times be applied to replace the injection locking system.

Funding. National Natural Science Foundation of China (NSFC) (61405107, 61227015, 61227902); Natural Science Foundation of Shanxi Province (Shanxi Province Natural Science Foundation) (2014021011-3); Scientific and Technological Innovation Programs of Higher Education Institution in Shanxi (2013104).

REFERENCES

1. K. I. Martin, W. A. Clarkson, and D. C. Hanna, Opt. Lett. **22**, 375 (1997).
2. S. Greenstein and M. Rosenbluh, Opt. Commun. **248**, 241 (2005).
3. H. D. Lu, J. Su, Y. H. Zheng, and K. C. Peng, Opt. Lett. **39**, 1117 (2014).
4. H. D. Lu, X. J. Sun, M. H. Wang, J. Su, and K. C. Peng, Opt. Express **22**, 24551 (2014).
5. H. D. Lu and K. C. Peng, J. Quantum Opt. **21**, 171 (2015).
6. A. E. Amili and M. Alouini, Opt. Lett. **40**, 1149 (2015).
7. T. C. Ralph, C. C. Harb, and H. A. Bachor, Phys. Rev. A **54**, 4359 (1996).
8. J. Zhang, Y. L. Cheng, T. C. Zhang, K. S. Zhang, C. D. Xie, and K. C. Peng, J. Opt. Soc. Am. B **17**, 1695 (2000).
9. C. W. Zhang, H. D. Lu, Q. W. Yin, and J. Su, Appl. Opt. **53**, 6371 (2014).
10. C. C. Harb, T. C. Ralph, E. H. Huntington, I. Freitag, D. E. McClelland, and H. A. Bachor, Phys. Rev. A **54**, 4370 (1996).